An Electromagnetic Simulator for Sentinel-3 SAR Altimeter Waveforms Over Land—Part II: Forests

Giuseppina De Felice Proia, *Member, IEEE*, Marco Restano, Davide Comite, *Senior Member, IEEE*, Maria Paola Clarizia, *Senior Member, IEEE*, Jérôme Benveniste, Nazzareno Pierdicca, *Senior Member, IEEE*, and Leila Guerriero, *Member, IEEE*

***Abstract*— Forests play a crucial role in the climate change mitigation by acting as sinks for carbon and, consequently, reducing the CO_2 concentration in the atmosphere and slowing global warming. For this reason, above ground biomass (AGB) estimation is essential for effectively monitoring forest health around the globe. Although remote sensing-based forest AGB quantification can be pursued in different ways, in this work, we discuss a new technique for vegetation observation through the use of altimetry data that have been introduced by the ESA-funded ALtimetry for BIOMass (ALBIOM) project. ALBIOM investigates the possibility of retrieving forest biomass through Copernicus Sentinel-3 Synthetic Aperture Radar Altimeter (SRAL) measurements at the Ku- and C-bands in low- and high-resolution modes. To reach this goal, a simulator able to reproduce the altimeter acquisition system and the scattering phenomena that occur in the interaction of the radar altimeter pulse with vegetated surfaces has been developed. The Tor Vergata Vegetation Scattering Model (TOVSM) developed at Tor Vergata University has been exploited to simulate the contribution from the vegetation volume via the modeling of the backscattering of forest canopy through a discrete scatterer representation. A modification of the Soil And Vegetation Reflection Simulator (SAVERS) developed by the team for Global Navigation Satellite System Reflectometry over land has also been taken into account to simulate the soil contribution.**

***Index Terms*— Altimetry, forests, Sentinel-3, simulations.**

I. Introduction

ACCELERATING progress on monitoring and accounting carbon emissions is of paramount importance to deliver on net zero carbon commitments and to stabilize the global warming target temperature at or below 1.5°C by 2030 in line with the Paris Climate Agreement [1] and recently brought back to the headlines during the 26th United Nations Climate Conference (COP26) [2]. This goal is reachable if the crucial role of forests is considered. Over the last decades, the scientific community has recognized forest biomass as one of the essential climate variables (ECVs), fundamental in understanding carbon sources and sinks and in diminishing haziness in our awareness of the climate system [3]. Biomass can be estimated indirectly in different ways by means of remote sensing [4]. This has produced a large literature on biomass evaluation, yet it is commonly agreed that neither a single satellite nor an algorithm would provide the best assessment of worldwide biomass [5]. Relevant works have been recently proposed to better characterize the amounts and the spatial distribution of above-ground biomass (AGB), using optical and microwave sensors. AGB maps have been produced by integrating data from various satellite missions at different scales, but the validation of all these techniques suffers from a lack of adequate ground truth measurements [6], [7]. Moreover, despite this fundamental task, forest biomass is poorly quantified in most regions of the world; therefore, a rigorous investigation is needed to make best use of existing information, integrate various data sources, and improve large-area AGB estimation globally and with sufficient accuracy, including remote sensing instruments designed for other applications. In this context, the ALtimetry for BIOMass (ALBIOM) project (https://eo4society.esa.int/projects/albiom/) intends to retrieve forest biomass from the Copernicus Sentinel-3 (S-3) Synthetic Aperture Radar Altimeter (SRAL) data at the Ku- and C-bands, in low- and high-resolution modes [8]. In the present study, we explore the results reached by the electromagnetic simulator of S-3 SRAL altimeter measurements developed in ALBIOM over vegetated surfaces.

The review of the existing literature reports few works focused on altimetry backscatter over soil and shows highly promising correlation with vegetation-related parameters. Smith et al. [9] demonstrate the potential of altimetry for forest canopy measurements and the inadequacy of the Shuttle Radar Topography Mission (SRTM) digital elevation model (DEM) for this kind of scenario; profiles of altimetric backscatter along tracks over continents have been analyzed in [10], [11], and [12], reporting statistical analysis of spatial and temporal variations of backscattering for the main land types. Only qualitative descriptions of the waveforms collected over land [13], [14] have been found, with no specific exploitation of S-3 data over land for vegetation purposes. An exception is the study in [15] which focuses on S-3 SRAL echo simulation over complex terrains taking into account an empirical computation of the backscattering coefficient and a DEM.

Manuscript received 15 March 2022; revised 13 July 2022; accepted 31 August 2022. Date of publication 28 September 2022; date of current version 18 October 2022. This work was supported by the European Space Agency (ESA) under ALBIOM Contract 4000128825/19/I-DT. *(Corresponding author: Giuseppina De Felice Proia.)*

Giuseppina De Felice Proia and Leila Guerriero are with the Department of Civil Engineering and Information Engineering, Tor Vergata University of Rome, 00133 Rome, Italy (e-mail: giuseppina.de.felice.proia@uniroma2.it; leila.guerriero@uniroma2.it).

Marco Restano is with SERCO SpA, ESA-ESRIN, 00044 Frascati, Italy (e-mail: marco.restano@esa.int).

Davide Comite and Nazzareno Pierdicca are with the Department of Information Engineering, Electronics, Telecommunications, Sapienza University of Rome, 00184 Rome, Italy (e-mail: davide.comite@uniroma1.it; nazzareno.pierdicca@uniroma1.it).

Maria Paola Clarizia is with the European Space Agency, ESA-ESTEC, 2201 AZ Noordwijk, The Netherlands (e-mail: maria.paola.clarizia@esa.int).

Jérôme Benveniste is with the European Space Agency, ESA-ESRIN, 00044 Frascati, Italy (e-mail: jerome.benveniste@esa.int).

Digital Object Identifier 10.1109/TGRS.2022.3210722

In a companion paper [16], the model developed in ALBIOM for bare soil has been described, and the simulation results have been presented. Here, we extend the model to forested surfaces introducing the scattering function of vegetation that is calculated according to appropriate electromagnetic approximations. ALBIOM exploits the Tor Vergata Scattering Model (TOVSM) developed at Tor Vergata University to simulate the backscattering of a forest canopy through a discrete scatterer representation [17], [18], in order to mimic the contribution from the vegetation volume, and the model in [19] simulating the soil contribution through a modification of Soil And Vegetation Reflection Simulator (SAVERS) [20]. Furthermore, the model takes forest allometric equations into account (as, e.g., in [21]) which describe the relationship between the tree biomass and the tree geometric parameters.

II. S-3 Altimeter Simulator Over Forests

The altimetric simulator has been realized via a modification of the TOVSM and SAVERS simulators. TOVSM simulates the electromagnetic properties (scattering and extinction) of vegetation elements which are outlined through simple canonical shapes (disks and cylinders). SAVERS was designed to simulate GNSS-R signals from land surfaces, applying the bistatic radar equation and the Woodward impulse function to the bistatic scattering coefficient calculated through TOVSM. SAVERS has been adapted to the specific S-3 SRAL altimeter instrument through application of the appropriate impulse function, and also the nadir-looking configuration, as it has been described in detail in [16], considering the integral radar equation for the monostatic altimetric configuration. On its side, TOVSM has been used, up to now, to simulate the backscattering coefficient measured by conventional radar systems that transmit pulses (with duration in the order of microsecond) and receive the echoes backscattered by the illuminated targets that are resolved in the 2-dimensional (2-D) ground range/azimuth plane, with a single look resolution in the order of dozens of meters. To be applied in the altimeter configuration, TOVSM has been modified in order to provide σ^0 along the propagation path of the electromagnetic wave, i.e., the z vertical dimension (given the altimeter nadiral observation direction).

Indeed, the S-3 SRAL altimeter transmits pulses with a range resolution ($c/2B$), after pulse compression, of about 47 cm at the Ku-band (determined by the speed of light c and the useful bandwidth B = 320 MHz at the Ku-band), thus giving the possibility to resolve the targets along the third dimension. To reach the same range resolution, TOVSM has taken advantage of the matrix doubling algorithm at its own basis.

The simulation of altimeter waveforms from forests is realized through two steps. First, it is necessary to establish the backscattering coefficient of the crown layers interacting with the altimeter pulse along its propagation path. Second, the "layered" backscattering coefficient is integrated in the bistatic radar equation solved by SAVERS.

The bistatic scattering and extinction coefficient of vegetation are computed through the Tor Vergata model [22]. The latter is based on the solution of the radiative transfer equation for a medium made of randomly distributed scatterers representing the different vegetation elements, i.e., leaves, branches, and trunks. Their geometrical properties are reproduced through simple canonical shapes (disks and cylinders), to which the most suitable electromagnetic approximation can be applied (Physical Optics, Rayleigh-Gans, and Infinite Cylinder) depending on the frequency under study and on the scatterer size. The contributions from the various scattering and extinction sources are combined through the matrix doubling algorithm [23] that allows the inclusion of multiple scattering effects of any order that take place between vegetation elements themselves, and between vegetation and terrain. In this study, the features of matrix doubling have been exploited to simulate the scattering coefficient along the propagation path through the vegetation layer. Due to the very high vertical range resolution, as the pulse propagates through the crown, the altimeter sees the scattering coefficient of one spherical shell at a time, where the incident and scattered power are attenuated by the aforementioned vegetation. As the pulse propagates, the radius of the spherical shell increases (top of Fig. 1), and this effect is simulated adding an elemental layer at a time, as in the bottom line of Fig. 1. Of course, the attenuation increases as the number of encountered elemental layers increases. Through the matrix doubling, it is possible to calculate the backscattering coefficient of each elemental layer, adding the contribution from one elemental layer at a time. In its new altimetric version, TOVSM stores into a lookup table (LUT) the backscattering coefficient of each elemental layer during each step of the matrix doubling algorithm [23].

The LUT will then be used as input to SAVERS. The LUT basically reports σ^0 versus tree height at the different vegetation depths inside the canopy. For the purpose of this study, it is more convenient to speak about σ^0 as a function of the lag, where the lag #1 is the one associated with the vegetation layer first met by the altimeter pulse, the lag #2 is the second one, and so on. The lag order N pertaining to the soil depends on the forest tree height. We mention that σ^0(N) is the backscattering coefficient of the whole forest canopy, and it is added to soil backscattering once the pulse reaches the ground. Additionally, σ^0(N) contains scattering contributions from interactions between the various scattering sources, i.e., multiple scattering between leaves, branches, and soil. We finally remark that the soil contribution, present from lag #N on, is included taking into account both the soil coherent quasi-specular reflection and the incoherent bistatic scattering component. Both are implemented in SAVERS and are attenuated by the above-lying vegetation.

SAVERS is able to model the range (time) delay τ_{ij} between the altimetric signal received from any point on the observed surface (x_j, y_i) and the one received from the subsatellite point on the ellipsoid τ_0, considering a DEM = $f(x,y)$. On its basis, SAVERS evaluates the delay $\tau_{\text{soil}ij}$ for each surface point (x_j, y_i) [16]. When a forest covered area is to be studied, a second DEM is calculated that takes into account the tree height (h)

$$\text{DEM}_{\text{veg}} = f(x, y) + h \tag{1}$$

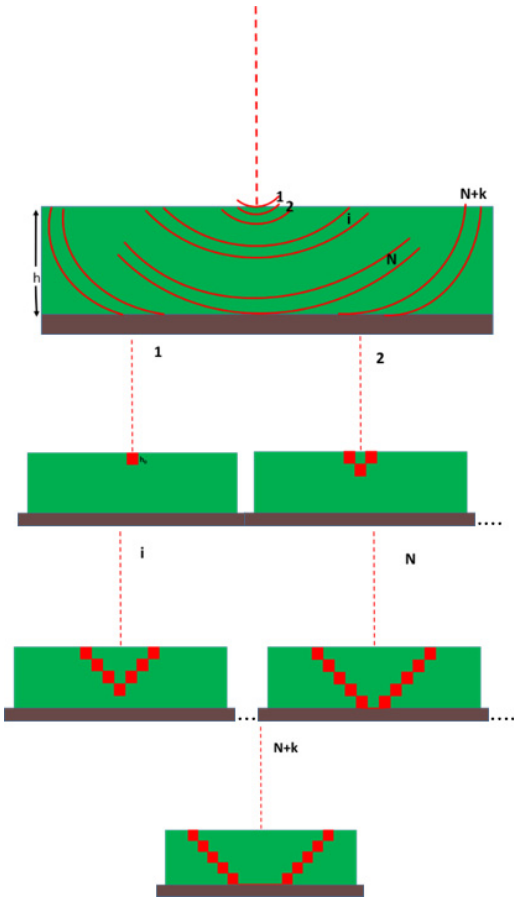

Fig. 1. Sketch in the vertical plane of interactions between the incident electromagnetic wave and the forest canopy, at different instances of time. (Top) Propagation of altimeter pulse at different instances of time. (Bottom) Corresponding geometric approximation in the TOVSM model.

which is obtained by simply adding the forest height to the surface DEM. In other words, given a certain forest height, it is assumed that the observed area is covered by a homogeneous forest, and the local topographic features are maintained. In the current version of SAVERS, the tree height value must be given as input, and it must be chosen among seven values considered for the generation of the LUT, i.e., $h = 10$, 15, 17, 19, 21, 22, and 23 m.

For each point on the surface, an additional delay $\tau_{\text{veg}ij}$ is calculated. Therefore, for each surface element with coordinates (x_j, y_i), two delays, $\tau_{\text{soil}ij}$ and $\tau_{\text{veg}ij}$, are compared with the sample delay τ', and then used to calculate the impulse response function.

An example of the forest effect is reported in Fig. 2 for the case of a surface without any topography (a synthetic flat surface). The tallest tree shows a wider waveform, since the return from the top of canopy is closer to the altimeter. It also shows a higher return from shorter delays and lower return from larger ones. This is due to the higher backscattering of the forest with larger biomass (taller trees) and to the higher attenuation of the soil contribution (present at larger delays). The attenuation itself is the reason of the decreasing value of the peak power versus the tree height. Both the incoherent and the coherent components characterize the backscattering coefficient of the altimeter because of its nadir configuration

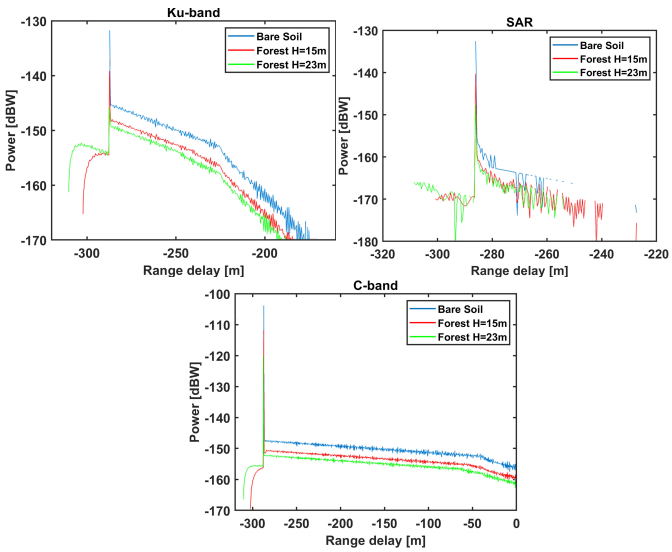

Fig. 2. Simulated waveform of a synthetic flat surface for the case of bare soil (blue), forest with tree height = 15 m (red) and 23 m (green). A soil roughness $\sigma_z = 0.5$ cm has been used. (Top left) LRM Ku-band, (top right) SAR Ku-band, and (bottom) LRM C-band.

(see [24, Fig. 5.30]), but according to model simulations, when the surface is very smooth as in the case of the synthetic flat example, the soil coherent scattering is so large that incoherent scattering is negligible. Even in the presence of trees with 23 m height, the attenuated soil coherent component at nadir ($\sim$148 dBW) is larger than the incoherent scattering from both vegetation and soil ($<$150 dBW). It is worth mentioning that incoherent scattering, from both soil and vegetation, is basically constant in the small range of angles involved in the altimeter observations.

Simulations of SAR mode were performed according to the procedure described in [16]. They show lower values of returned power in a restricted range of delays (Fig. 2, top right plot), because of the reduced integration area. Note that the peak power at nadir is unchanged with respect to Ku-band LRM (Fig. 2, top-left plot), thus showing that coherent scattering contribution is provided by the facets just surrounding the nadir point. On the contrary, C-band simulations provide higher signal power in a wider range of delays (Fig. 2, bottom plot). Given the same roughness parameters, the surface appears smoother at the C-band, thus returning higher power at nadir. The lower frequency allows a deeper penetration inside the canopy, i.e., the power undergoes a lower attenuation by vegetation. Finally, because of the largest antenna beamwidth at the C-band, a decrease of 6 dB is observed at a farther range delay (up to -50 m at the C-band against -230 m at the Ku-band).

III. Comparison With S-3 SRAL Waveforms Over Central African Forests

The validation of SAVERS simulator for S-3 SRAL for vegetated surfaces has been realized over different kinds of African forests. The dataset (enhanced L2 products [25]) that has been downloaded from the European Space Agency (ESA) Copernicus Open Access Hub includes the 20-Hz high-resolution data vector at the Ku-band [synthetic aperture

TABLE I

APRIL 2017 ACQUISITIONS: COORDINATES SELECTED OVER THE ORBIT NO. 99 AND ALTIMETER TRACKING MODE

SCENARIO	COORDINATES	ASCENDING S-3A SRAL No. ORBIT	SENSING DATE	TRACKING MODE
Central African Republic site no. 1	Lat=8.9902° Lon=19.1942°	99	1st April 2017	Open loop
Central African Republic site no. 2	Lat=8.1109° Lon=19.3920°	99	1st April 2017	Open loop

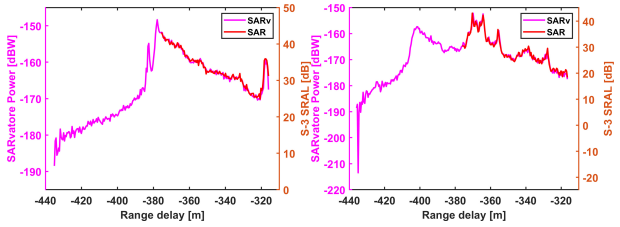

Fig. 3. Comparison between SAR waveforms in official Copernicus S-3 (in red, "SAR") and SARvatore (in magenta, "SARv") products collected over site #1 (left) and site #2 (right).

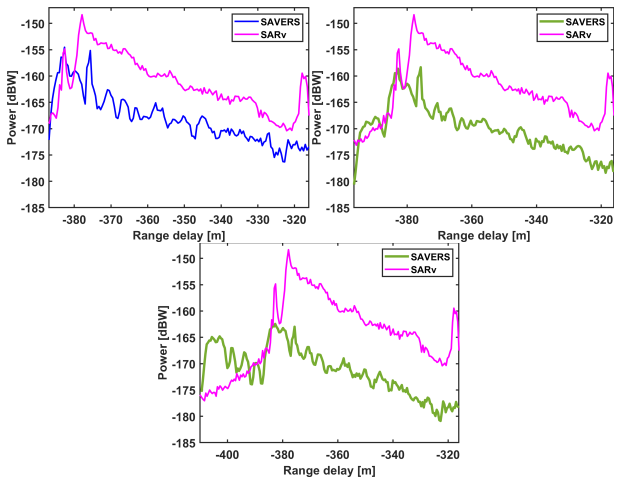

Fig. 4. Comparison of SAVERS and SARvatore waveforms at site #1. (Top left) Bare soil simulation, (top right) simulation for forest height = 10 m, and (bottom) simulation for forest height = 23 m. A manual shift of −4 m has been applied on the modeled waveform.

radar (SAR) mode], the pseudo-low-resolution data vector at the Ku-band [pseudo-low-resolution mode (PLRM)], and the data at the C-band [low-resolution mode (LRM)]. Alternative S-3 20-Hz SAR data made available through the ESA G-POD SAR Versatile Altimetric Toolkit for Ocean Research & Exploitation (SARvatore) for S-3 service [26] have also been considered to compare with the aforementioned official S-3 Copernicus SAR data. Specifically, the SARvatore for S-3 service allows the users to customize the processing at L1b (SAR processing) and L2 (retracking) by setting a list of configurable options, not available in the official operational processing chains, and can also provide SAR waveforms over a selectable range of delay (receiving window) that can be extended up to 512 lags. Additionally, the collected power is made available in dBW units, so that the comparison of the magnitude of the measured and simulated power is allowed. This is not possible with the official S-3 Copernicus data which include the power in FFT power units (https://sentinel.esa.int/web/sentinel/technical-guides/sentinel-3-altimetry/appendices/faq, see FAQ-Altimetry-003).

Primarily, some waveforms acquired during the S-3A ascending track no. 99 in April 2017 were selected. Along this track, the altimeter collects data, among others, over the Central African Republic, a region characterized by the presence of several kinds of land covers such as herbaceous vegetation, shrubland, and mainly forest. Two coordinates along the track have been selected with the aid of Google images which display a variable amount of green vegetation in the area and are reported in Table I. For each of them, the altimeter tracking mode [27] given in the S-3 L2 products is also reported.

In the present work, we realize an alignment between the simulated and the experimental waveforms exploiting the S-3 SRAL L2 product nominal tracking gate (i.e., bin indexed as 44 and 46 in the Ku- and C-bands, respectively). The S-3 range delay has been calculated following the procedure described in [16, Sec. III].

Fig. 3 reports a comparison between SAR waveforms in Copernicus S-3 and SARvatore products. The Copernicus S-3 SAR waveforms have been aligned to the last 128 bins of the SARvatore waveforms. The Copernicus S-3 data collected over forest do not reproduce all the peaks of SARvatore waveforms, and they show a clear truncation that misses the leading edge. This crucial aspect of waveform truncation has been investigated in the sensitivity analysis of S-3 SRAL waveform to biomass, as preliminary work was carried out in the ALBIOM project [28], and it is due both to an incorrect positioning of the time-tracking window that may be positioned referring to the previous target not suitable to cover the entire waveform in the current altimeter position (we remark that the altimeter is working in the open-loop mode over both coordinates according to Table I), and to its insufficient length (i.e., $128 \times 0.47 = 60$ m) over land. This may be a drawback, especially over forests where the region likely related to volume scattering associated with vegetation creates a return that is not properly allocated within the receiving window. Indeed, in most of the examples that we are going to show, earlier peaks in SARvatore waveforms are associated with the signal coming from the top of canopy, and the later peaks are related to the reflection from the ground at nadir, as reported for the ranging scatterometer [29].

After this preliminary observation, SARvatore waveforms have been compared with the simulated waveforms. We have considered three different cases of SAVERS simulations, that is, bare soil, forest characterized by small trees, and forest with tall trees. The comparisons between SAVERS simulations and SARvatore waveforms are shown, respectively, in Fig. 4, for the site no. 1, and in Fig. 5, for the site no. 2. To better match the S-3 waveform, a shift of the SAVERS waveform might be considered, as highlighted in [16]. For the first scenario, we can appreciate better similarities in case of bare soil through a manual alignment with a shift of –4 m of the SAVERS waveform (Fig. 4, left). For the second scenario, it is possible

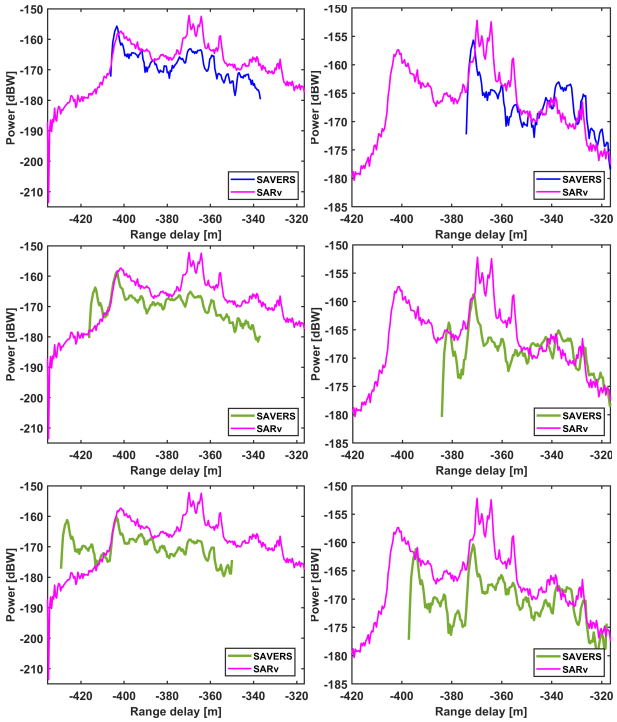

Fig. 5. Comparison of SAVERS and SARvatore waveforms at site #2. (Top) Bare soil simulation, (middle) simulation for forest height = 10 m, and (bottom) simulation for forest height = 23 m. (Left column) alignment according to S-3 waveform bin #44 and (right column) ad hoc manual shift of 32 m of the modeled waveform.

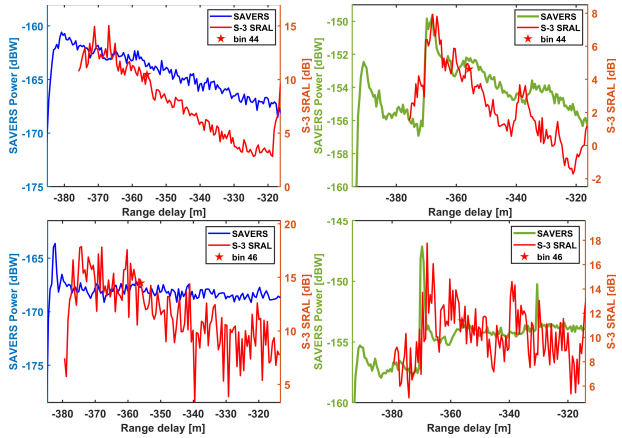

Fig. 6. Comparison of SAVERS simulations and official Copernicus S-3 waveforms. (Top row) Ku PLRM waveform. (Bottom row) C-band. (Left column) Site #1. (Right column) Site #2. Green: forest simulation using tree height = 23 m; blue: bare soil simulation; and red: S-3 SRAL waveforms in Copernicus official products.

TABLE II

VALUES OF THE APPLIED SHIFTS WITH RESPECT TO THE TRACKING BIN # 44 (46) OVER THE SELECTED SCENARIOS

SCENARIO	COORDINATES	Shift LRM Ku-band [m]	Shift SAR Ku-band [m]	Shift C-band [m]
Central African Republic site no. 1	Lat=8.9902° Lon=19.1942°	3.1	-4	-2.5
Central African Republic site no. 2	Lat=8.1109° Lon=19.3920°	35	32	35

to reach a good alignment with the experimental waveform (Fig. 5, bottom right) applying a shift of 32 m on the SAVERS waveform for a forest characterized by tall trees.

As a consequence of this visual interpretation that takes into account the slope of the leading and trailing edges, we make the hypothesis that the area observed by the altimeter at the geographic locations of the first scenario is not covered by vegetation, whereas the second scenario is covered by tall trees. These hypotheses will be further discussed with reference to Fig. 7, where images acquired by Sentinel-1 SAR are used as ancillary data.

In general, we observe that the simulated waveforms reproduce quite well the SARvatore waveform shape, although the experimental power values are underestimated. As discussed in [16], the inclusion of multi-look processing, planned as a future improvement of SAVERS for simulations of S-3 high resolution measurements, could improve the results of the comparisons over the studied scenarios. Additionally, in this study, we have fixed the tree parameters (i.e., branch, trunk, and leaf sizes and their orientation) on the basis of allometric equations that are quite generic. This allows a comprehensive view of the altimetric response, but some local characteristics of forests may not be well represented. An unrealistic reproduction of the attenuation and scattering properties of the forest elements could yield the gap between simulations and data observed in Fig. 5.

The considerable shift applied to obtain a good alignment between experimental and simulated waveforms depends on an incorrect elevation provided by the SRTM DEM over vegetated surfaces, and it will be discussed in Section IV.

In Fig. 6, we have compared the SAVERS simulations with, respectively, the Ku-band PLRM and C-band LRM official S-3 data. The simulated waveforms in green or in blue are linked to the previous alignments, through which the range delay of the ground and the height of trees has been established and represent, respectively, bare soil and forest. To account for the variability of the area involved in the footprint at the C-band, we have introduced different values of terrain roughness with respect to the 0.5 cm characterizing Ku-band scenarios [16]. Both the PLRM and the C-band cases require an ad hoc shift of SAVERS waveforms, as reported in Table II.

As previously mentioned, we will discuss this issue in Section IV. Here, we conclude showing ancillary information that supports our hypothesis of different cover types in the two geographic regions taken into account for the model validation.

We analyzed the Sentinel-1 (S-1) SAR L1 products acquired in March 2021 over the Central African Republic [30]. The sensor acquires data with a 250 km swath at 5 m by 20 m spatial resolution (single look) [31]. We have considered the ground range detected (GRD) data in interferometric wide (IW) swath mode—the main acquisition mode over land—referring to the sum of co-polarization and cross-polarization (i.e., VV + HV). The 20 km × 20 km patch (according to the altimeter footprint) multi-looked at 100 m has been taken into account over the two examined scenarios.

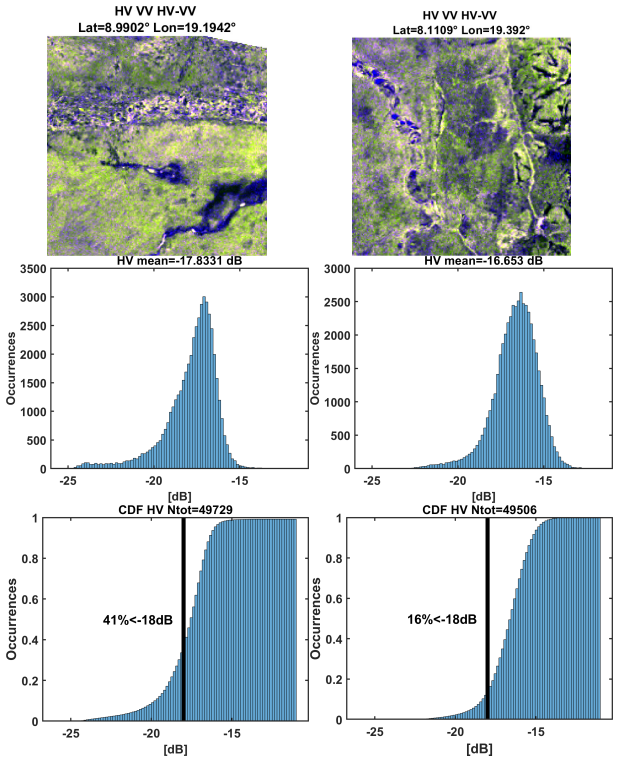

Fig. 7. S-1 SAR image cuts of 20 km × 20 km around altimeter nadir, and multilooked at 100 m over the two selected scenarios in Central African Republic (top) in RGB composition: HV, VV, HV-VV; (middle) HV polarization histograms; and (bottom) HV polarization CDF histograms.

Fig. 7 (top) reports the RGB image centered on each of the two coordinates, and combining HV, VV, and HV–VV polarizations. Fig. 7 (middle) reports the histogram of HV acquisitions, and Fig. 7 (bottom) reports the corresponding cumulative distribution function (CDF). It is well known that low cross-polarized backscattering coefficients are associated with bare soil, while significant cross-polarization is introduced by vegetation. The histogram of the first coordinate is more asymmetric and skewed toward lower values rather than the histogram of the second coordinate. This peculiarity is also apparent in the CDFs where a backscattering coefficient threshold of –18 dB has been enhanced by a black bar: the first coordinate shows the highest percentage of pixels with backscattering coefficient lower than –18 dB, so that the SAR data in Fig. 7 support the identification of forest and bare soil obtained from the altimeter waveforms.

We finally point out that the identification of forest and bare soil from the waveforms is confirmed by the Global Land cover map at 100 m resolution for the year 2017 provided by Copernicus Land Monitoring Service [32].

IV. Role of DEM Error Over Forests

A. SRTM DEM

The meaning of the shift parameter used in the previous waveform alignment has been clarified in [16]. In summary, when the SRTM DEM does not correctly reproduce the real topography, a difference occurs between the experimental range delay and the SAVERS one, and it introduces a mismatch in the alignment between the waveforms. In other words, the shift represents the difference between real topography and the DEM; that is, the error of SRTM. The latter is quite small for the bare soil scenario (i.e., Central African Republic site no. 1), much larger for forest scenario (i.e., Central African Republic site no. 2). Indeed, the literature recognizes that, when complex media are considered, interferometric SAR measurements are not able to clearly locate the ground level; typically, it happens whenever the ground is covered by vegetation or trees [33]. In this case, the interferometric phase refers to an elevation placed somewhere between ground and tree top depending on forest density and wavelength. This is the case of DEMs produced by radar sensors at higher frequencies, such as SRTM [34] or Tandem-X [35], in which attenuation and scattering by dense forest canopies can cause biases. The proposed forested scenario could correspond to very dense forest canopies, where SRTM DEM shows the inability of the Shuttle Radar to penetrate the forest and reach the ground, so the elevation provided could be affected by vertical errors between 10 and 40 m [36], [37], [38]. It is worth mentioning that the shifts reported in Table II and applied to the forest simulation are positive shifts, thus supporting the hypothesis of a bad evaluation of the surface height by SRTM DEM.

B. Lidar Digital Terrain Model

In order to reduce the error introduced by the SRTM DEM, we have considered a vegetated area in Gabon (West Africa), where a digital terrain model was available.

The selection of the coordinates has been carried out among the data offered by the Africa SAR (AfriSAR) mission, an airborne campaign that collected lidar, radar, and field measurements of tropical forests in Gabon from 2010 to 2016 [39], [40]. The region represents a mix of forested, savannah, and some agricultural and disturbed landcover types in four sites: Lopé, Mabounie, Mondah, and Rabi. For each AfriSAR site, a digital terrain model (DTM) and a canopy height model (CHM), built at 1-m resolution, are also made available along with georeferenced polygons, as shown in [41]. Because of the proximity to the Atlantic Ocean of Mondah and Rabi sites, and the absence of S-3 SRAL tracks over the Lopé site, only Mabounie region has been taken into account in this study. S-3B ascending track no. 242 collected in March 2019 has been considered.

First of all, a comparison between the histograms of the SRTM DEM and DTM over Mabounie coordinates [Fig. 8 (top) and (center), respectively) has been carried out. The difference of the mean surface elevations reaches 26 m that corresponds approximately to the mean tree height of the site provided by the CHM, that is, 28.6 m (Fig. 9), thus confirming the error of the SRTM DEM over vegetated areas.

Then, a histogram matching technique has been applied on the SRTM DEM patch over Mabounie, using as reference the Mabounie DTM histogram [Fig. 8 (bottom)]. Comparing the histograms at the top and bottom of Fig. 8, it is possible to observe that the matching method has produced a reduction

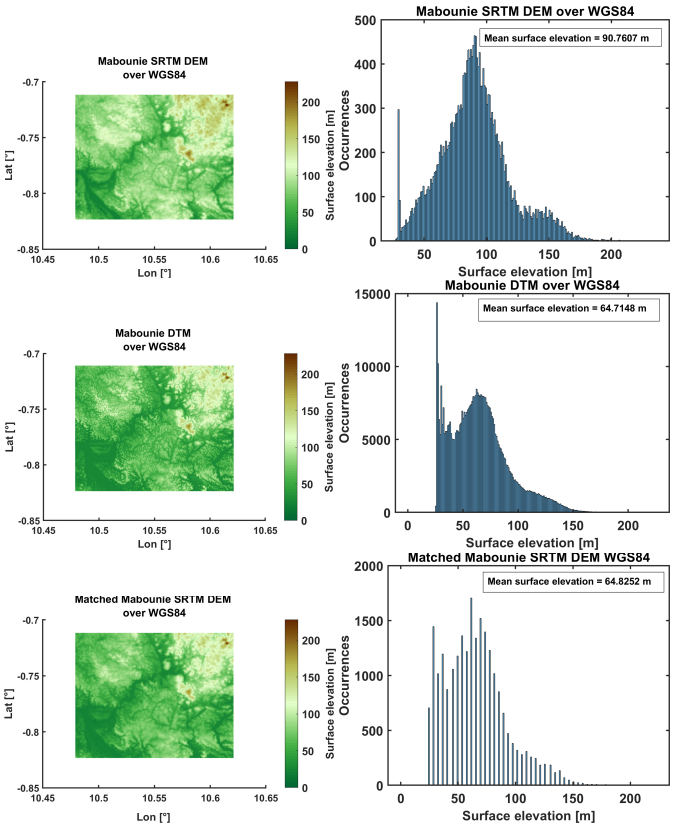

Fig. 8. (Top) SRTM DEM over WGS84 at Mabounie site (left); histogram of the SRTM DEM over WGS84 at Mabounie site (right). (Center) DTM over WGS84 at Mabounie site (left); histogram of the DTM over WGS84 at Mabounie site (right). (Bottom) Matched SRTM DEM over WGS84 at Mabounie site (left); histogram of the matched SRTM DEM over WGS84 at Mabounie site (right).

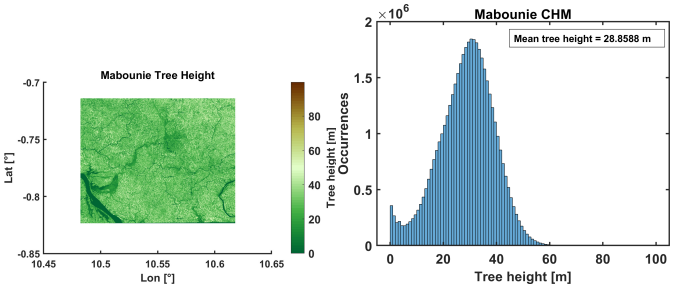

Fig. 9. (Left) Canopy height model at Mabounie site and (right) histogram of the CHM at Mabounie site.

of the original surface elevation of about 26 m. In order to exploit this technique in the simulations, we have processed the 5° × 5° SRTM DEM tiles obtaining matched tiles to be given as input to SAVERS.

Two coordinates along the track have been selected and are reported in Table III. For each scenario, we have processed the simulated waveforms without and with the histogram matching method, considering in both cases a tree height of 23 m. This technique has been considered in the following for the high-resolution waveforms only, but it can be extended to the low-resolution case at both the Ku- and C-bands.

TABLE III

SELECTED COORDINATES ALONG THE S-3B TRACK NO. 242 OVER MABOUNIE

SCENARIO	COORDINATES	ASCENDING S-3B SRAL No. ORBIT	SENSING DATE	TRACKING MODE
Mabounie site no. 3	Lat=-0.7600° Lon=10.6089°	242	24th March 2019	Open loop
Mabounie site no. 4	Lat=-0.7194° Lon=10.5999°	242	24th March 2019	Open loop

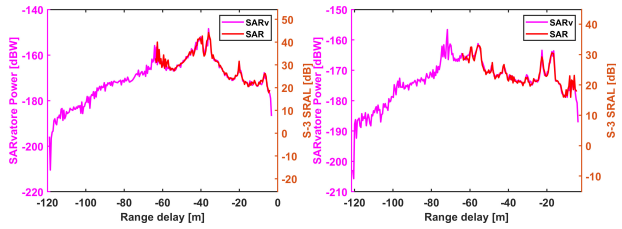

Fig. 10. Comparison among L2 waveforms and SARvatore waveforms collected over site #3 (left) and site #4 (right).

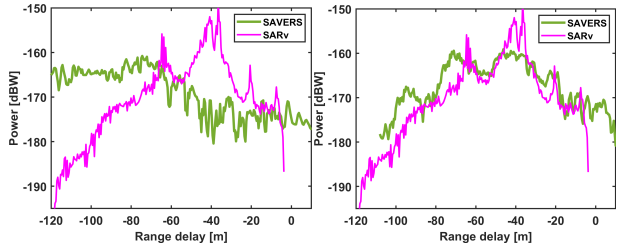

Fig. 11. Comparison of SAVERS simulations and SARvatore waveforms at site #3. (Left) Simulation for forest height = 23 m and original SRTM DEM as input. (Right) Simulation for forest height = 23 m and matched SRTM DEM as input with an ad hoc shift of 8 m.

Fig. 10 reports a comparison between Copernicus and SARvatore waveforms at the two selected coordinates. As seen for the vegetated scenarios over the Central African Republic, the Copernicus official data collected over forests do not always reproduce all the peaks in the SARvatore waveform and may show the truncation of the leading edge.

The comparisons between SAVERS simulations and SARvatore waveforms at the coordinate of the site no. 3 are reported without and with the histogram matching in Fig. 11. We can appreciate good similarities through the use of the histogram matching in the simulation shifted by 8 m with respect to the S-3 tracking.

Satisfactory similarities are also reached thanks to the histogram matching in the simulation over the coordinate of the site no. 4 (Fig. 12). An ad hoc shift of 9 m has been applied.

We point out that the necessity of the small shift and the remaining gap both in the vertical dynamics and in the waveform shape in Fig. 11 (right) and Fig. 12 (right) are probably due to the small size of the available DTM used in the histogram matching with respect to the size of the DEM which is required by the simulator.

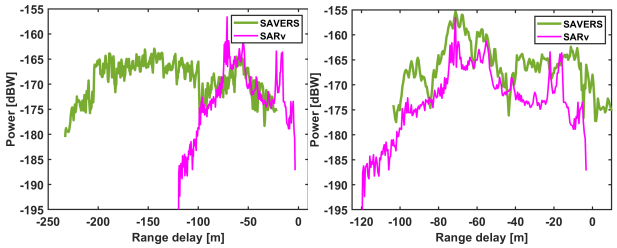

Fig. 12. Comparison of SAVERS simulations and SARvatore waveforms at site #4. (Left) Simulation for forest height = 23 m and original SRTM DEM as input. (Right) Simulation for forest height = 23 m and matched SRTM DEM as input with an ad hoc shift of 9 m.

V. Conclusion

The work presents the modeling method adopted to simulate the altimeter measurements over vegetated scenarios. Merging SAVERS and TOVSM, the waveforms of bare soil and forest covered surfaces have been modeled. The role of topography has also been considered, as well as low- and high-resolution data, at the Ku- and C-bands. Once a general description of the simulator skills has been given, a comparison with S-3 SRAL data has been carried out. For this purpose, not only the official ESA Copernicus data but also the waveforms from the ESA G-POD SARvatore for S-3 service have been exploited. The GPOD products offer a much larger range dynamics of the waveforms (i.e., 512 bins) which is quite convenient to analyze the data, especially when the correspondent official Copernicus waveforms appear truncated. Indeed, this is often the case for the acquisitions over forested areas.

The simulations related to forested surfaces provide waveforms with at least two peaks, due to the top of canopy and to the ground. The presence of topography may further introduce other peaks in the waveforms, making the identification of vegetation and topographic effects very challenging. Indeed, a waveform that was initially identified as "forest" waveform was finally connected to bare soil after comparison with simulations. Despite the composite patterns, the developed simulator proved its capability to reproduce the main characteristics of the S-3 waveforms. In particular, the slope of the trailing edge is generally well reproduced for each case examined, as well as the power of the SARvatore waveforms. However, the range delay alignment between SAVERS simulations and S-3 range delays produced by means of the nominal tracking gate does not work well over forest scenarios. These cases call for a large shift in the range of the simulated waveform (on the order of 30 m), which seems to be necessary to get a better reproduction of the waveforms acquired over forest areas. To explain the range mismatch, we made the hypothesis that the SRTM DEM included in the simulator to evaluate the range delay was not enough accurate over areas covered with vegetation. This is a well-known problem of DEMs elaborated from radar interferometry, and for this reason, a lidar DTM available from the AfriSAR campaign was used as a benchmark. The simulation results obtained using a DEM matched over this DTM provided encouraging results supporting the requirement of a reliable map of terrain elevation in forested area.

Acknowledgment

The authors would like to thank the entire ESA-ESRIN RSS GPOD Team for carrying out the SAR Altimetry processing. Users of the GPOD/SARvatore family of altimetry processors are supported under the coordination of Jérôme Benveniste (ESA-ESRIN) with ESA funding. S-3 data were provided by the European Space Agency as input to the GPOD/SARvatore service. Recently, the SARvatore family of services has been moved from ESA GPOD to the new Earth Console platform and can be accessed at: https://earthconsole.eu/. Many thanks also to the S-3 Ground Segment for clarifications provided throughout the project.

A final thanks to Dr. Nicolas Barbier—from IRD/UMR AMAP, Botanique et Modélisation de l'Architecture des Plantes et des végétations Montpellier, France—for providing very useful data from the AfriSAR Campaign.

References

[1] UNFCCC—PARIS AGREEMENT. (2015). *United Nations Framework Convention on Climate Change*. Accessed: Dec. 16, 2021. [Online]. Available: https://unfccc.int/process-and-meetings/the-paris-agreement/the-paris-agreement

[2] UNFCCC—Glasgow Climate Change Conference. (2021). *Outcomes of the Glasgow Climate Change Conference—Advance Unedited Versions (AUVs)*. Accessed: Dec. 16, 2021. [Online]. Available: https://unfccc.int/process-and-meetings/conferences/glasgow-climate-change-conference-october-november-2021/outcomes-of-the-glasgow-climate-change-conference

[3] S. Bojinski, M. Verstraete, T. C. Peterson, C. Richter, A. Simmons, and M. Zemp, "The concept of essential climate variables in support of climate research, applications, and policy," *Bull. Amer. Meteorolog. Soc.*, vol. 95, no. 9, pp. 1431–1443, 2014.

[4] I. H. Woodhouse, E. T. A. Mitchard, M. Brolly, D. Maniatis, and C. M. Ryan, "Radar backscatter is not a 'direct measure' of forest biomass," *Nature Climate Change*, vol. 2, no. 8, pp. 556–557, Aug. 2012.

[5] ESA, Eogateway News. (Jun. 7, 2018). *Copernicus Sentinels to Help Measure Earth's Biomass—News*. Accessed: Dec. 16, 2021. [Online]. Available: https://earth.esa.int/eogateway/news/copernicus-sentinels-to-help-measure-earths-biomass

[6] V. Avitabile et al., "An integrated pan-tropical biomass map using multiple reference datasets," *Global Change Biol.*, vol. 22, no. 4, pp. 1406–1420, 2016.

[7] J. M. B. Carreiras et al., "Coverage of high biomass forests by the ESA BIOMASS mission under defense restrictions," *Remote Sens. Environ.*, vol. 196, pp. 154–162, Jul. 2017.

[8] M. P. Clarizia et al., "Recent results from the ALBIOM project on biomass estimates from Sentinel-3 altimetry data," in *Proc. EGU Gen. Assem. Conf. Abstr.*, 2021, p. 12180.

[9] R. G. Smith, P. A. M. Berry, and J. Benveniste, "ACE2 validation and future look," in *20 Years of Progress in Radar Altimatry*, vol. 710, 2013.

[10] F. Papa, B. Legrésy, and F. Rémy, "Use of the Topex–Poseidon dual-frequency radar altimeter over land surfaces," *Remote Sens. Environ.*, vol. 87, nos 2–3, pp. 136–147, 2003.

[11] F. Frappart et al., "Radar altimetry backscattering signatures at Ka, ku, C, and S bands over West Africa," *Phys. Chem. Earth, A/B/C*, vols. 83–84, pp. 96–110, Jan. 2015.

[12] F. Frappart et al., "Backscattering signatures at Ka, Ku, C and S bands from low resolution radar altimetry over land," *Adv. Space Res.*, vol. 68, no. 2, pp. 989–1012, Jul. 2021.

[13] B. Legresy, F. Papa, F. Remy, G. Vinay, M. van den Bosch, and O.-Z. Zanife, "ENVISAT radar altimeter measurements over continental surfaces and ice caps using the ICE-2 retracking algorithm," *Remote Sens. Environ.*, vol. 95, no. 2, pp. 150–163, Mar. 2005.

[14] E. O. Pereira and P. Maillard, "The effect of land cover type on radar altimeter response and its influence on retracker algorithms," *Proc. SPIE*, vol. 9239, pp. 31–43, Oct. 2014.

[15] Z. Zhu, H. Zhang, and F. Xu, "Raw signal simulation of synthetic aperture radar altimeter over complex terrain surfaces," *Radio Sci.*, vol. 55, no. 2, Feb. 2020, Art. no. e2019RS006948.

[16] G. De Felice Proia et al., "An electromagnetic simulator for Sentinel-3 SAR altimeter waveforms over land—Part I: Bare soil," *IEEE Trans. Geosci. Remote Sens.*, vol. 60, no. 1, Oct. 2022, Art. no. 2007211.
[17] P. Ferrazzoli and L. Guerriero, "Passive microwave remote sensing of forests: A model investigation," *IEEE Trans. Geosci. Remote Sens.*, vol. 34, no. 2, pp. 433–443, Mar. 1996.
[18] P. Ferrazzoli, L. Guerriero, N. Pierdicca, and R. Rahmoune, "Forest biomass monitoring with GNSS-R: Theoretical simulations," *Adv. Space Res.*, vol. 47, no. 10, pp. 1823–1832, 2010.
[19] D. Comite, F. Ticconi, L. Dente, L. Guerriero, and N. Pierdicca, "Bistatic coherent scattering from rough soils with application to GNSS reflectometry," *IEEE Trans. Geosci. Remote Sens.*, vol. 58, no. 1, pp. 612–625, Jan. 2020.
[20] N. Pierdicca, L. Guerriero, R. Giusto, M. Brogioni, and A. Egido, "SAVERS: A simulator of GNSS reflections from bare and vegetated soils," *IEEE Trans. Geosci. Remote Sens.*, vol. 52, no. 10, pp. 6542–6554, Oct. 2014.
[21] J. C. Jenkins, D. C. Chojnacky, L. S. Heath, and R. A. Birdsey, "National-scale biomass estimators for United States tree species," *Forest Sci.*, vol. 49, pp. 12–26, Feb. 2003.
[22] M. Bracaglia, P. Ferrazzoli, and L. Guerriero, "A fully polarimetric multiple scattering model for crops," *Remote Sens. Environ.*, vol. 54, no. 3, pp. 170–179, Dec. 1995.
[23] H. J. Eom and A. K. Fung, "A scatter model for vegetation up to Ku-band," *Remote Sens. Environ.*, vol. 15, no. 3, pp. 185–200, Jun. 1984.
[24] F. T. Ulaby and D. G. Long, "Radar scattering," in *Microwave Radar and Radiometric Remote Sensing*. Ann Arbor, MI, USA: Univ. Michigan, 2014, ch. 5, p. 197.
[25] ESA, Preparation and Operations of the Mission Performance Centre (MPC) for the Copernicus Sentinel-3 Mission. (Apr. 29, 2020). *Product Data Format Specification—SRAL/MWR Level 2 Land Products*. Accessed: Feb. 16, 2022. [Online]. Available: https://sentinel.esa.int/documents/247904/2753172/Sentinel-3-Product-Data-Format-Specification-Level-2-Land
[26] J. Benveniste, S. Dinardo, G. Sabatino, M. Restano, and A. Ambrozio, "SAR altimetry processing on demand for CRYOSAT-2 and SENTINEL-3 using the ESA research and service support," in *Proc. Conf. Big Data Space (BiDS)*, Luxembourg, U.K., 2019, p. 1.
[27] S. Le Gac, F. Boy, D. Blumstein, L. Lasson, and N. Picot, "Benefits of the open-loop tracking command (OLTC): Extending conventional nadir altimetry to inland waters monitoring," *Adv. Space Res.*, vol. 68, no. 2, pp. 843–852, Jul. 2021.
[28] D. Comite et al., "Estimating biomass from Sentinel-3 altimetry data: A sensitivity analysis," in *Proc. IEEE Int. Geosci. Remote Sens. Symp.*, Jul. 2021, pp. 2389–2392.
[29] J. Hyyppa and M. Hallikainen, "A helicopter-borne eight-channel ranging scatterometer for remote sensing. II. Forest inventory," *IEEE Trans. Geosci. Remote Sens.*, vol. 31, no. 1, pp. 170–179, Jan. 1993.
[30] ESA. (2022). *Sentinel Online, User Guides, Sentinel-1 SAR, Level-1*. Accessed: Jan. 23, 2022. [Online]. Available: https://sentinel.esa.int/web/sentinel/user-guides/sentinel-1-sar/product-types-processing-levels/level-1
[31] ESA. (2022). *Sentinel Online, User Guides, Sentinel-1 SAR, Interferometric Wide Swath*. Accessed: Jan. 23, 2022. [Online]. Available: https://sentinel.esa.int/web/sentinel/user-guides/sentinel-1-sar/product-types-processing-levels/level-1
[32] (2022). *VITO Remote Sensing. Global Land Cover 2017*. Accessed: Jan. 23, 2022. [Online]. Available: https://lcviewer.vito.be/2017
[33] M. M. D'Alessandro, S. Tebaldini, and F. Rocca, "Phenomenology of ground scattering in a tropical forest through polarimetric synthetic aperture radar tomography," *IEEE Trans. Geosci. Remote Sens.*, vol. 51, no. 8, pp. 4430–4437, Aug. 2012.
[34] J. E. Belz, E. Rodriguez, and C. S. Morris, "A global assessment of the SRTM performance," *Photogramm. Eng. Remote Sens.*, vol. 72, no. 3, pp. 249–260, 2006.
[35] B. Wessel, M. Huber, C. Wohlfart, U. Marschalk, D. Kosmann, and A. Roth, "Accuracy assessment of the global TanDEM-X digital elevation model with GPS data," *ISPRS J. Photogramm. Remote Sens.*, vol. 139, pp. 171–182, May 2018.
[36] J. Kellndorfer et al., "Vegetation height estimation from shuttle radar topography mission and national elevation datasets," *Remote Sens. Environ.*, vol. 93, no. 3, pp. 339–358, Nov. 2004.
[37] C. C. Carabajal and D. J. Harding, "ICESat validation of SRTM C-band digital elevation models," *Geophys. Res. Lett.*, vol. 32, no. 22, pp. 1–5, 2005.
[38] R. G. Smith and P. A. M. Berry, "Evaluation of the differences between the SRTM and satellite radar altimetry height measurements and the approach taken for the ACE2 GDEM in areas of large disagreement," *J. Environ. Monit.*, vol. 13, no. 6, pp. 1646–1652, 2011.
[39] ESA. (2016). *AfriSAR 2016: Technical Assistance for the Development of Airborne SAR and Geophysical Measurements During the AfriSAR Experiment*. Accessed: Jan. 23, 2022. [Online]. Available: https://earth.esa.int/eogateway/campaigns/afrisar-2016?text=afrisar&category=Campaigns
[40] AfriSAR. *DAAC Home, Get Data, NASA Projects*. Accessed: Jan. 23, 2022. [Online]. Available: https://daac.ornl.gov/cgi-bin/dataset_lister.pl?p=382018
[41] N. Labriere et al., "*In situ* reference datasets from the TropiSAR and AfriSAR campaigns in support of upcoming spaceborne biomass missions," *IEEE J. Sel. Topics Appl. Earth Observ. Remote Sens.*, vol. 11, no. 10, pp. 3617–3627, Oct. 2018.

Giuseppina De Felice Proia (Member, IEEE) received the master's degrees (*cum laude*) in telecommunications engineering, two specializations in teaching computer science and in teaching to students with disabilities, respectively, from the University of Cassino and Southern Lazio, Cassino, Italy, in 2011 and 2015, respectively, and the University of Roma Tre, Rome, Italy, in 2018. She is currently pursuing the Ph.D. degree in geoinformation with the University of Rome "Tor Vergata," Rome.

In 2011, she joined MBDA Italia S.p.A., Rome, within international remote sensing defense programs for two years. Since 2013, she has been working as an Upper Secondary School Computer Science Teacher with MIUR, Rome. From 2020 to 2022, she collaborated with the IIA-CNR, Rome, through a fellowship within the ISTC-CNR Advanced School in Artificial Intelligence. She has participated in the ESA projects ALBIOM and HydroGNSS. Her research interests include SAR altimetry, electromagnetic modeling, and artificial intelligence applied to Earth observation and climate change.

Ms. De Felice Proia is a member of the IEEE Geoscience and Remote Sensing Society and the IEEE Women in Engineering.

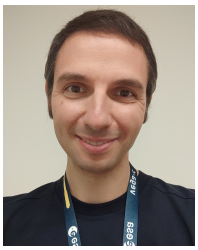

Marco Restano received the M.Sc. degree (*cum laude*) in telecommunications engineering and the Ph.D. degree in radar remote sensing from the Sapienza University of Rome, Rome, Italy, in 2009 and 2014, respectively.

He performed research activities oriented to Mars exploration with ESA/MEX MARSIS and NASA/MRO SHARAD ground-penetrating radars which included the study of wave scattering and propagation into ionospheric and stratified mediums. In 2015, he led an Italian–American effort together with NASA/JPL, USA; Smithsonian Institution, USA; and Southwest Research Institute, USA; to evaluate the effects of the passage of Comet C/2013 A1 (Siding Spring) observed by the Shallow Radar (SHARAD) on Mars Reconnaissance Orbiter. In 2015, he joined the Altimetry Team at the European Space Agency Earth Observation Centre, Frascati, Rome. In 2016, he developed an alternative processor for the compensation of ionospheric effects in MARSIS signals. He deals with altimetry processing algorithm development for the exploitation of CryoSat-2, Sentinel-3, and Sentinel-6 SAR altimetry missions and their application to Earth System Science, supports many ESA Research and Development contracts in the "Earth Observation for Society" Program and in the ESA "Climate Change Initiative," gave many lectures to teach radar altimetry, and is a coauthor of many publications.

Davide Comite (Senior Member, IEEE) received the master's degree (*cum laude*) in telecommunications engineering and the Ph.D. degree in electromagnetics and mathematical models for engineering from the Sapienza University of Rome, Rome, Italy, in 2011 and 2015, respectively.

He is currently a tenure-track Assistant Professor with the Sapienza University of Rome. He was a visiting Ph.D. student at the Institute of Electronics and Telecommunications of Rennes, University of Rennes 1, Rennes, France, in 2014, and a Post-Doctoral Researcher with the Center of Advanced Communications, Villanova University, Villanova, PA, USA, in 2015. His scientific interests involve Earth observation, remote sensing, study of the scattering from natural surfaces, GNSS reflectometry over land, radar altimetry for biomass monitoring, study and design of microwaves and millimeter-waves antennas, antenna arrays, leaky waves, leaky-wave antennas, and the generation of non-diffracting waves and pulses.

Dr. Comite was a recipient of awards at both national and international conferences. He received the IEEE Antennas and Propagation Society Outstanding Reviewer Award for the IEEE TRANSACTIONS ON ANTENNAS AND PROPAGATION, in 2019, 2020, and 2021. In 2020, he was awarded as the Best Reviewer for the IEEE JOURNAL OF SELECTED TOPICS IN APPLIED EARTH OBSERVATION AND REMOTE SENSING. He is an Associate Editor of the IEEE JOURNAL OF SELECTED TOPICS IN APPLIED EARTH OBSERVATION AND REMOTE SENSING, the *EurAAP Journal Reviews of Electromagnetics*, the *IET Journal of Engineering*, the *IET Microwaves, Antennas and Propagation* by the Institution of Engineering and Technology, and IEEE ACCESS. Since November 2020, he has been one of officers of the Young Professional Affinity Group of the IEEE Italian Chapter. Since January 2021, he has been leading the GNSS-R Modeling Working Group of the GRSS MIRS Technical Committee. Since March 2022, he has been the Chair of the ECAP Working Group of EuRAAP. He is a Union Radio Scientifique Internationale - International Union of Radio Science (URSI) Senior Member.

Maria Paola Clarizia (Senior Member, IEEE) received the master's degree in telecommunications engineering from the University of Sannio, Benevento, Italy, in 2007, and the Ph.D. degree in ocean remote sensing using GNSS-Reflectometry (GNSS-R) from the University of Southampton, Southampton, U.K., in 2012.

She has more than 15 years of experience in remote sensing, with a focus on GNSS-R, working in both academia and private industry. She worked as a Post-Doctoral Research Fellow with the University of Michigan, Ann Arbor, MI, USA, on the NASA CYGNSS Mission, being a core member of the CYGNSS science team, and responsible for the baseline wind speed retrieval algorithm of the mission itself. She has also been the Head of the GNSS-R Group, Deimos Space U.K., Didcot, U.K., working on a variety of projects involving GNSS-R for land and ocean applications. She is currently a Wave Interaction and Propagation Engineer at HE Space, Noordwijk, The Netherlands, for the European Space Agency (ESA), supervising projects and activities, and providing support to GNSS-R and synthetic aperture radar (SAR) satellite missions. Her expertise and research interests include GNSS-Reflectometry, altimetry, scatterometry, SAR, electromagnetic scattering models, end-to-end simulations, retrieval algorithms, data analysis, and statistical processing.

Jérôme Benveniste received the Ph.D. degree in oceanography from space from the University of Toulouse, Toulouse, France, in 1989.

After a post-doctoral in space data assimilation in ocean models at MIT, Boston, MA, USA, he moved to the European Space Agency (ESA). Since 1992, he has been with the ESA Earth Observation Data Center, Rome, Italy, where he is the In-Charge of the ERS-1, ERS-2, ENVISAT, CryoSat, Sentinel-3, and Sentinel-6 radar altimetry data exploitation. He interacts with ESA principal investigators, organizes scientific symposia, and regularly launches research and development projects, including GOCE data exploitation. He was recognized as a Senior Advisor at ESA in 2008. He is a Co-Editor of a book on *Coastal Zone Radar Altimetry* (Springer, 2011). He is an editor of a peer-reviewed scientific journal and a guest-editor of five journal special issues. He launched and monitors the Climate Change Initiative Sea Level Project (2009) and its current sequel focused on the coastal zone, as well as other projects on sea level budget closure, runoff, river discharge, ocean heat content, Easter boundary upwelling systems, coastal oceanography, and coastal hazards.

Nazzareno Pierdicca (Senior Member, IEEE) received the Laurea (Doctor's) degree (*cum laude*) in electronic engineering from the Sapienza University of Rome, Rome, Italy, in 1981.

From 1978 to 1982, he was with the Italian Agency for Alternative Energy (ENEA), Italy. From 1982 to 1990, he was with the Remote Sensing Division, Telespazio, Rome. In November 1990, he joined the Department of Information Engineering, Electronics and Telecommunications, Sapienza University of Rome, where he is a full Professor and teaches remote sensing, antennas, and electromagnetic fields with the faculty of engineering. He is the past Chairperson of the GRSS Central Italy Chapter. His research interests include electromagnetic scattering and emission models for sea and bare soil surfaces and their inversion, microwave radiometry of the atmosphere, and radar land applications.

Leila Guerriero (Member, IEEE) received the Laurea degree in physics from the Sapienza University of Rome, Rome, Italy, in 1986, and the Ph.D. degree in electromagnetism from the Tor Vergata University of Rome, Rome, in 1991.

Since 1994, she has been a Permanent Researcher with Tor Vergata University, where she is currently an Associate Professor holding the courses on earth satellite observation and geoinformation. Her research interests include modeling microwave scattering and emissivity from agricultural and forested areas. She participated in several international projects, among them: the ESA projects Soil Moisture and Ocean Salinity Satellite; Development of SAR Inversion Algorithms for Land Applications; Use of Bistatic Microwave Measurements for Earth Observation; and SAOCOM-CS Bistatic Imaging, Radiometry and Interferometry Over Land. She has been involved in the modeling of Global Navigation Satellite System Reflectometry (GNSS-R) signals for ESA projects and in the European FP7 and H2020 Programs.